

## Degradation of dye on polyoxotungstate nanotube under molecular oxygen

Fang Chai <sup>a,b</sup>, Lijuan Wang <sup>c</sup>, Linlin Xu <sup>a</sup>, Xiaohong Wang <sup>a,\*</sup>, Jiguo Huang <sup>c,\*</sup>

<sup>a</sup> Institute of Polyoxometalate Chemistry, Department of Chemistry, Northeast Normal University, Changchun 130024, PR China

<sup>b</sup> Department of Chemistry, Harbin Normal University, Harbin 150500, PR China

<sup>c</sup> College of Environment and Resources, Jilin University, Changchun 130026, PR China

Received 13 June 2005; received in revised form 17 August 2006; accepted 17 August 2006

Available online 1 November 2006

### Abstract

A facile process to prepare polyoxometalate  $\text{Zn}_{1.5}[\text{PW}_{12}\text{O}_{40}]$  nanotube is presented. The structure and morphology of this nanotube were characterized using IR, elemental analyses, X-ray powder diffraction,  $^{31}\text{P}$  MAS NMR and transmission electron microscopy. This nanotube material has a self-supporting tube structure that can be used as a heterogeneous catalyst for the degradation of safranin T (ST) using molecular oxygen (air) as oxidant and can be easily separated from the aqueous phase, thus enabling it to be used several times.

© 2006 Elsevier Ltd. All rights reserved.

**Keywords:** Polyoxometalate; Nanotube; Synthesis; Catalyst; Degradation of organic dye

### 1. Introduction

Polyoxometalates (POMs) constitute a large class of inorganic compounds with considerably potential applications in catalysis, medicine and material sciences [1–3]. The self-assembly of such POM building blocks to produce multifunctional materials is becoming a rapidly expanding area of research [4], owing to their unique structural versatility and electronic properties. By far, the most important application of POMs is the field of catalysis, particularly the selective oxidation of industrial materials and products [2,3]. Recently, they have also been applied as environmental catalysts for the photodegradation of various organic pollutants [5], and also applied for wet air oxidation (WAO) [6] of organic pollutants. However, few studies have been made to develop polyoxometalate catalyst for the direct activation of molecular oxygen in the degradation of organic pollutants.

Recently, many efforts have been made using “advanced oxidation technologies” (AOT) for the treatment of recalcitrant

pollutants to more biodegradable molecules or mineralization into  $\text{CO}_2$  and other inorganics [7]. So  $\text{H}_2\text{O}_2$ ,  $\text{O}_3$  and molecule oxygen (air) have been widely used as green oxidants in organic synthesis and environmental remediation because of their green byproduct and high content of active oxygen species [8]. Many POMs have been confirmed to be effective catalysts for activating  $\text{H}_2\text{O}_2$ ,  $\text{O}_3$  and molecular oxygen in selected oxidation of various organic substrates in dark thermal reactions [8–13]. Compared with  $\text{H}_2\text{O}_2$ , molecular oxygen (air) is cheaper agent in industrial use which exhibits academic value as well as commercial value. The development of an efficient catalytic system for direct activation of molecular oxygen is of great interest.

Because of the high solubility of POMs in aqueous media, some research groups have put forward many efforts for the recovery and reuse of POMs. To achieve this, there are two approaches: one is to implant POMs onto a solid support leading to a catalytic system that may be filtered and reused [14]; the second is to use biphasic liquid–liquid systems, such that at separation temperatures, the catalyst and product phases may be separated by phase separation [15–18]. In the first method, the simple way is to change the soluble catalysts

\* Corresponding authors.

E-mail address: [Wangxh665@nenu.edu.cn](mailto:Wangxh665@nenu.edu.cn) (X. Wang).

into insoluble bulk materials, which in some cases dissolve under reaction conditions. Our group has systematically investigated the synthesis of nanoscale POMs using biological templates such as liposome, or starch microspheres [19,20]. The biological template method is proven to be a flexible way to control the size, structure and higher order organization of inorganic framework [21–23]. As a continuation of our work, we explored to synthesize 1D POM nanotubes using biological template – cellulose fibers associated with surface sol–gel process. This way is suitable for large scale and industrial preparations.

We report here the synthesis of POM  $\text{Zn}_{1.5}\text{PW}_{12}\text{O}_{40}$  nanotubes and their application as heterogeneous catalysts for the degradation of safranin T using molecular oxygen (air) as oxidation agent. The structure of ST is shown in Scheme 1, which is a dye mixture of two compounds. Color removal has become a challenging aspect of textile wastewater treatment because of the growing concern about residual color that is closely associated with toxicity and aesthetics of the discharged effluent [24]. Most commonly practiced physical–chemical methods such as coagulation, activated carbon adsorption, membrane filtration and aerobic biological treatment have been proven to be inefficient for decolorization [25] due to dyes' high degree of chemical, photolytic and microbial stabilities.

This is the first report on the synthesis of POM nanotubes using natural cellulose template and is being used as an oxide catalyst for the degradation of organic dyes utilizing molecular oxygen.

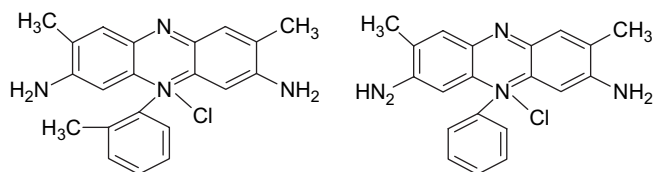
## 2. Experimental

### 2.1. Materials

$\text{H}_3\text{PW}_{12}\text{O}_{40}$  was prepared according to literature methods and identified by IR spectra and elemental analyses [26]. Ethanol and zinc acetate were purchased from Aldrich and used without further treatment. All other reagents were of AR grade.

### 2.2. Physical measurements

Elemental analyses of  $\text{Zn}_{1.5}\text{PW}_{12}\text{O}_{40}$  were carried out using a Leeman Plasma Spec (I) ICP-ES. IR spectra (2000–400  $\text{cm}^{-1}$ ) of the nanotubes were recorded in KBr discs on a Nicolet Magna 560 IR spectrometer. The clear filtrate solution of the catalytic process was tracked by UV–vis spectroscopy using a 756 CRT UV–vis spectrophotometer at 532 nm.



Scheme 1. The molecular structure of ST.

Electron micrographs were recorded on a Hitachi H-600 transmission electron microscope. NMR spectra were recorded on a Unity-400 spectrometer at room temperature. The X-ray powder diffraction (XRD) patterns (Fig. 2) of the sample were collected on Japan Rigaku Dmax 2000 X-ray diffractometer with  $\text{Cu K}\alpha$  radiation ( $\lambda = 0.154178 \text{ nm}$ ).

### 2.3. Preparation of catalyst $\text{Zn}_{1.5}\text{PW}_{12}\text{O}_{40}$ nanotubes

$\text{H}_3\text{PW}_{12}\text{O}_{40} \cdot 23\text{H}_2\text{O}$  (8 g, 2.4 mmol) was dissolved in 20 mL distilled water to form a clear solution. This solution was added dropwise into 10 mL ethanol solution containing 1.6 g, 7.2 mmol zinc acetate with gentle stirring. The final pH of this mixture was 2. The mixture was continuously stirred for about 30 min, then some pieces of filter paper were dipped into this solution for 15 min and then the filter paper was thoroughly washed with water and ethanol in order to remove the POM complex and zinc acetate which did not attach into the filter paper surface. Then the filter paper coated with  $\text{Zn}_{1.5}\text{PW}_{12}\text{O}_{40}$  was dried by airflow. This procedure was repeated for 20 times. The resultant paper/ $\text{Zn}_{1.5}\text{PW}_{12}\text{O}_{40}$  complexes were calcined in air to remove the original filter paper. The greenish-yellow powder which was self-supporting was obtained with yield of 40 mg.

### 2.4. Catalytic procedure

The stoichiometry of reaction was determined by allowing 34.1 mg/L of ST to react with air at room temperature in the presence of the catalyst. A general procedure was carried out as follows: 0.2 g of catalyst  $\text{Zn}_{1.5}\text{PW}_{12}\text{O}_{40}$  nanotube was suspended in a fresh aqueous dye solution ( $C_0 = 34.1 \text{ mg/L}$ , 200 mL). The air was inputted into the bottom of the suspension with the flow being  $0.08 \text{ m}^3/\text{h}$ . At given intervals of illumination, a sample of suspension was taken out by filtration. UV–vis spectroscopy was used in the experiment to monitor the degradation of ST.

## 3. Results and discussion

### 3.1. Preparation

In the previous reports, the POMs with nanostructure were synthesized by carbon-nanotube template, nonionic inverse microemulsion, surfactant template, etc. To the best of our knowledge, there is no report using natural cellulosic substances as template to fabricate nanoscale POMs. The surface sol–gel process could be explained as that a solid substrate with hydroxyl groups on its surface is allowed to react with metal alkoxides in solution to form covalently bound surface monolayers of the metal alkoxides and subsequent hydrolysis. The natural cellulose fibers possess hydroxyl groups on the surface, so the sol–gel process can occur on the surface of cellulose [22,23]. It is known that metal alkoxides are expensive and unstable which the sol–gel process is difficult to be controlled. We attempted using simple inorganic metal salts as a precursor to achieve the sol–gel process. The procedure

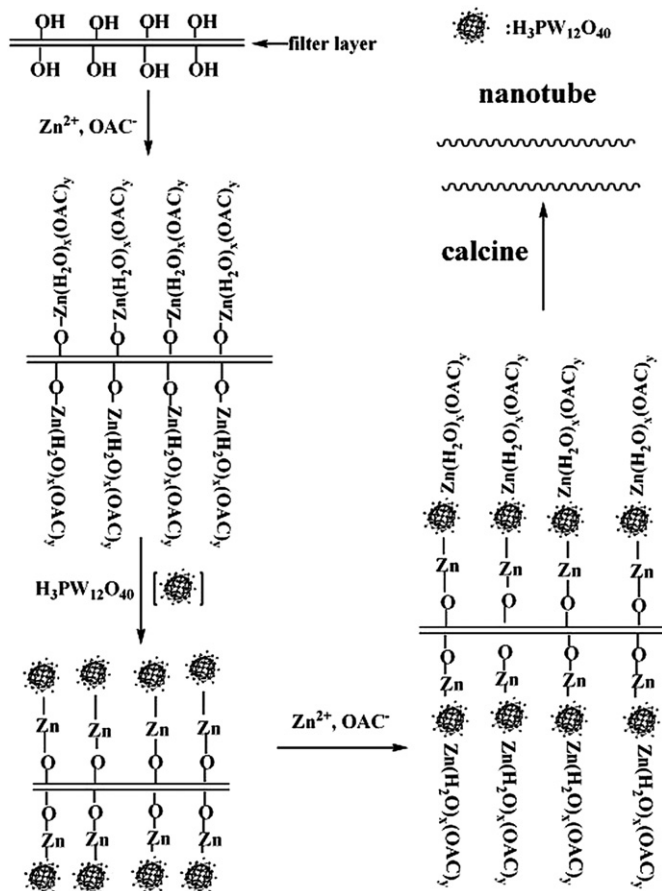


Fig. 1. The formation of Zn<sub>1.5</sub>PW<sub>12</sub>O<sub>40</sub> nanotubes.

of formation of cellulosic fiber covered by Zn<sub>1.5</sub>PW<sub>12</sub>O<sub>40</sub> can be observed in Fig. 1.

### 3.2. Elemental results

From the result of elemental analysis, the contents of the material are W, 75.9; P, 1.0; Zn, 3.2%, and it can be seen that while the POMs were forming the nanotubes, the ratio of W:P:Zn is 12:1:1.5 corresponding to the formula of Zn<sub>1.5</sub>PW<sub>12</sub>O<sub>40</sub>.

### 3.3. Spectra

The IR spectrum of the Zn<sub>1.5</sub>PW<sub>12</sub>O<sub>40</sub> nanotubes was in good agreement with that of its parent PW<sub>12</sub>O<sub>40</sub><sup>3-</sup> observed in macro-scale, with the four characteristic peaks reflecting the different vibrations of oxygen atoms of the Keggin-type structure PW<sub>12</sub>O<sub>40</sub><sup>3-</sup>: 1083, 987, 895 and 810 cm<sup>-1</sup> could be attributed to the asymmetry vibrations P–O<sub>a</sub> (internal oxygen connecting P and W), W–O<sub>d</sub> (terminal oxygen bonding to W atom), W–O<sub>b</sub> (edge-sharing oxygen connecting W) and W–O<sub>c</sub> (corner-sharing oxygen connecting W<sub>3</sub>O<sub>13</sub> units).

The XRD of the Zn<sub>1.5</sub>PW<sub>12</sub>O<sub>40</sub> nanotubes is shown in Fig. 2. All the diffraction peaks in Fig. 2 could be readily indexed to tetragonal PW<sub>12</sub>O<sub>40</sub> phase (JCPDS no. 41-0369).

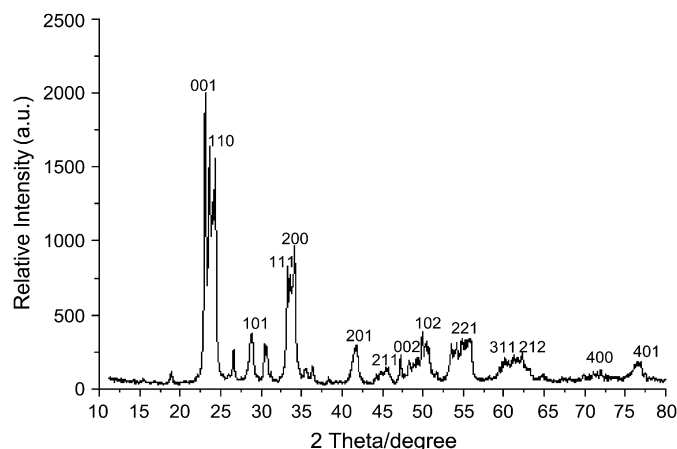


Fig. 2. XRD pattern of the Zn<sub>1.5</sub>PW<sub>12</sub>O<sub>40</sub> nanotubes.

These results indicate that the heteropolyanion in the as-prepared nanotubes retains its original Keggin-type molecular structure.

In order to further confirm the structure of Zn<sub>1.5</sub>PW<sub>12</sub>O<sub>40</sub> nanotubes, the <sup>31</sup>P MAS (magic-angle spinning) NMR spectrum of the sample (Fig. 3) was analyzed. It displayed a characteristic peak at –14.9 ppm, which is as same as the starting H<sub>3</sub> PW<sub>12</sub>O<sub>40</sub> (–15.0 ppm) [27], suggesting that during the synthetic process, the POMs PW<sub>12</sub>O<sub>40</sub> keep its structure. The slight shift may be due to the change of counteranions.

### 3.4. Morphology of the material

The morphology and microstructure of the prepared Zn<sub>1.5</sub>PW<sub>12</sub>O<sub>40</sub> were investigated with transmission electron microscopy (TEM). Typical TEM image (Fig. 4) showed that the sample displayed tube-like shapes. As shown in Fig. 4, some materials have the morphology of tube, in which middle cellulosic fibers have been burnt out to form the hollow tubes. The average length of the tubes is about 150 nm, and the width of the tubes is about 25 nm, the inner width being about 9 nm.

### 3.5. Degradation of ST

We studied the degradation of ST as a model reaction to investigate the oxidative-catalytic activity of Zn<sub>1.5</sub>PW<sub>12</sub>O<sub>40</sub> under molecular oxygen at room temperature which was

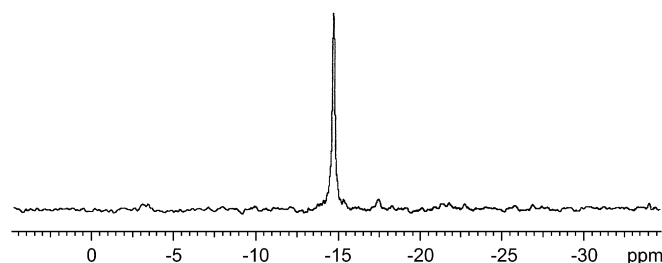


Fig. 3. The <sup>31</sup>P MAS NMR of Zn<sub>1.5</sub>PW<sub>12</sub>O<sub>40</sub> nanotubes.

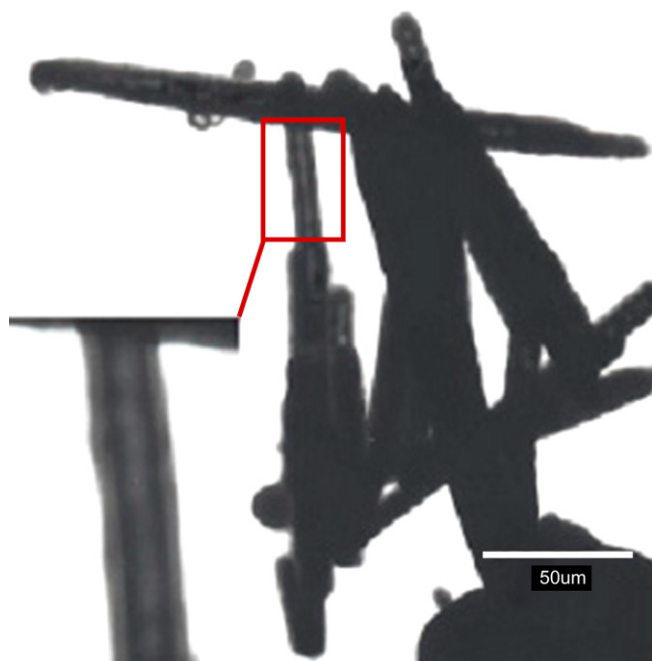


Fig. 4. The typical TEM image of the  $\text{Zn}_{1.5}\text{PW}_{12}\text{O}_{40}$  nanotubes.

determined by UV–vis spectra at 532 nm. The concentration changes of ST under different flowing air times are shown in Fig. 5. From Fig. 5, it can be seen that in the presence of catalyst  $\text{Zn}_{1.5}\text{PW}_{12}\text{O}_{40}$  nanomaterials, ST dye was decomposed by molecular oxygen. The decomposed rate reached 78% after flowing air for about 4 h.

In order to determine the catalytic effect of  $\text{Zn}_{1.5}\text{PW}_{12}\text{O}_{40}$  nanomaterials on dye's decolorization, different experiments were carried out as shown in Fig. 6. It can be seen that on flow air into the aqueous solutions of ST without any catalyst, ST did not degrade in the beginning of 0.5 h. On flowing air for 6 h, the degradation rate of ST only reached 32% (Fig. 6a). However, the conversion of ST was much higher when the catalyst  $\text{Zn}_{1.5}\text{PW}_{12}\text{O}_{40}$  nanomaterial was introduced into the mixture, i.e., the conversion of ST reached 80% after flowing air for 6 h. When the polyoxometalate  $\text{H}_3\text{PW}_{12}\text{O}_{40}$  without nanostructure was used (0.2 g) as catalyst, the ST

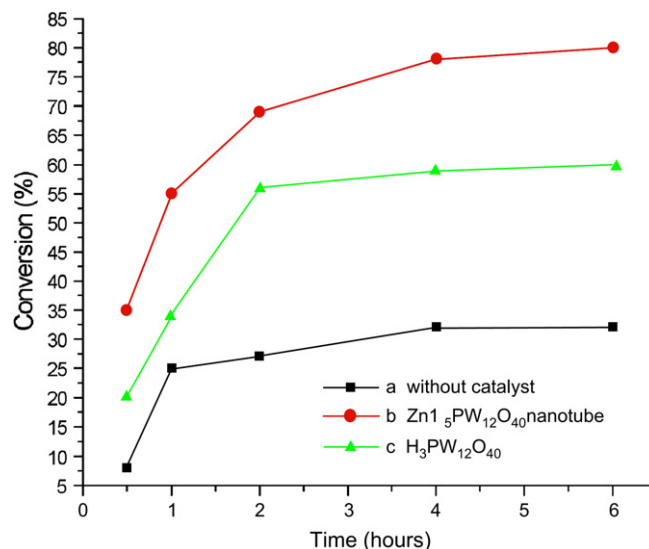


Fig. 6. Degradation of ST under different conditions.

conversion was less than 60% (Fig. 6c) in the same time, which shows that when forming nanotube structure, the BET surface area was augmented and the activity of it was improved.

After the reaction gets completed, the suspension was centrifuged, and the catalyst  $\text{Zn}_{1.5}\text{PW}_{12}\text{O}_{40}$  was separated. The amount of W determined by ICP-AES in the resulting clear solution was 0.1%, which confirmed the less solubility of the catalyst during the reaction process. The catalyst was reused for 4 times, during which the catalytic activity of  $\text{Zn}_{1.5}\text{PW}_{12}\text{O}_{40}$  in the degradation of ST was maintained efficiently with slightly decrease owing to the lesser dissolution (Fig. 7). And also the catalyst can be easily separated from the mixture.

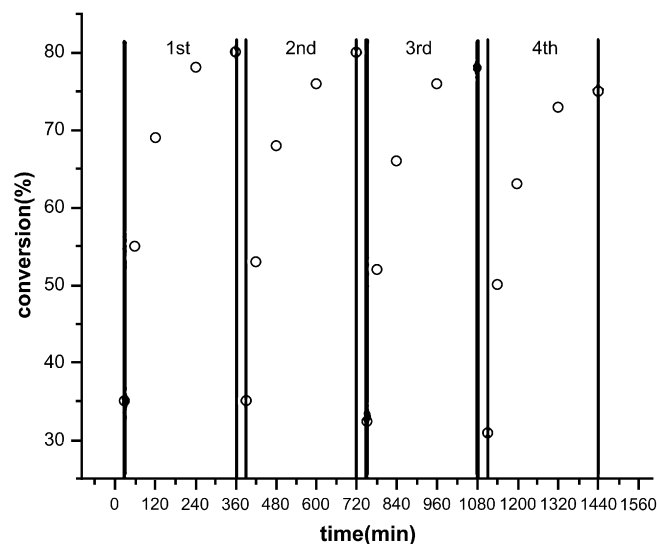


Fig. 7. Cycling runs in the oxidative-degradation of ST in the presence of  $\text{Zn}_{1.5}\text{PW}_{12}\text{O}_{40}$  under molecular oxygen.

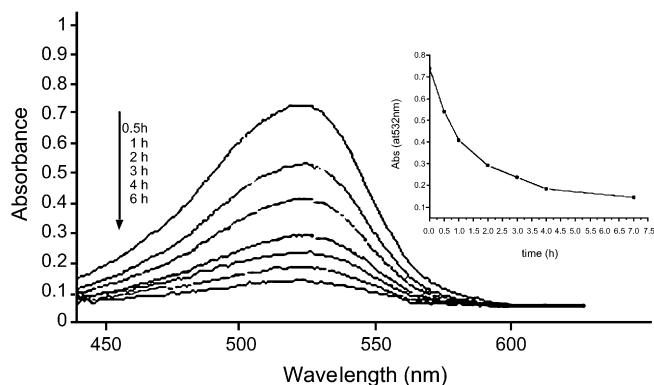


Fig. 5. The UV–vis absorption spectral changes of ST solution under catalyst with different flowing air times.

#### 4. Conclusion

Our ongoing research work shows that  $\text{Zn}_{1.5}\text{PW}_{12}\text{O}_{40}$  nanotubes could be prepared using cellulose fiber substance as templates associated with surface sol–gel method, which is a unique, convenient, low-cost and green chemical pathway. This method could be used not only to synthesize other POMs with 1D nanostructure, but also to enhance the surface area of the catalysts to increase the activity.  $\text{Zn}_{1.5}\text{PW}_{12}\text{O}_{40}$  nanotube is insoluble in water aqueous and can be used as a heterogeneous catalyst for degradation of safranin T using molecular oxygen (air) as oxidation agent. This catalytic process is a commercial and green chemical pathway which exhibits potential industrial application in dye's decolorization.

#### Acknowledgements

This work was supported by the National Natural Science Foundation of China (No. 39970842) and the Project Sponsored by the Scientific Research Foundation for the Returned Overseas Chinese Scholars, State Education Ministry (No. 201581).

#### References

- [1] Sun YG, Xia YN. Shape-controlled synthesis of gold and silver nanoparticles. *Science* 2002;298:2176–9.
- [2] Pope MT, Müller A. Polyoxometalate chemistry: an old field with new dimensions in several disciplines. *Angew Chem Int Ed Engl* 1991;30:34–8.
- [3] Müller A, Petters F, Pope MT, Gatteschi D. Polyoxometalates: very large clusters – nanoscale magnets. *Chem Rev* 1998;98:239–72.
- [4] Katsoulis DE. A survey of applications of polyoxometalates. *Chem Rev* 1998;98:359–88.
- [5] Lei PX, Chen CC, Yang J, Ma WH, Zhao JC, Zang L. Degradation of dye pollutants by immobilized polyoxometalate with  $\text{H}_2\text{O}_2$  under visible-light irradiation. *Environ Sci Technol* 2005;39:8466–74.
- [6] Gould D, Griffith W, Spiro M. Polyoxometalate catalysis of dye bleaching by hydrogen peroxide. *J Mol Catal A Chem* 2001;175:289–91.
- [7] Li J, Ma WH, Huang YP, Tao X, Zhao JC, Xu YM. Oxidative degradation of organic pollutants utilizing molecular oxygen and visible light over a supported catalyst of  $\text{Fe}(\text{bpy})_3^{2+}$  in water. *Appl Catal B Environ* 2004;48:17–24.
- [8] Xi Z, Zhou N, Sun Y, Li K. Reaction-controlled phase-transfer catalysis for propylene epoxidation to propylene oxide. *Science* 2001;292:1139–41.
- [9] Kamata K, Yonehara K, Sumida Y, Yamaguchi K, Hikichi S, Mixuno N. Efficient epoxidation of olefins with  $\geq 99\%$  selectivity and use of hydrogen peroxide. *Science* 2003;300:946–66.
- [10] Mizuno N, Nozaki C, Kiyoto I, Misono M. Highly efficient utilization of hydrogen peroxide for selective oxygenation of alkanes catalyzed by diiron-substituted polyoxometalate precursor. *J Am Chem Soc* 1998;120:9267–72.
- [11] Ishii Y, Yamawaki K, Ura T, Yamada H, Yoshida I, Ogawa H. Hydrogen peroxide oxidation catalyzed by heteropoly acids combined with cetylpyridinium chloride. Epoxidation of olefins and allylic alcohols, ketonization of alcohols and diols, and oxidative cleavage of 1,2-diols and olefins. *J Org Chem* 1988;53:3587–93.
- [12] Server-Carrio J, Bas-Serra J, Gonzalez-Nunez M, Garcia-Gastaldi A, Jameson G, Baker L, et al. Synthesis, characterization, and catalysis of  $\beta_3\text{[(Co}^{\text{II}}\text{O}_4\text{)W}_{11}\text{O}_{31}(\text{O}_2)_4]^{10-}}$  the first Keggin-based true heteropolydioxoxygen (peroxo) anion. Spectroscopic (ESR, IR) evidence for the formation of superoxo polytungstates. *J Am Chem Soc* 1999;121:977–84.
- [13] Neumann R, Gara M. Highly active manganese-containing polyoxometalate as catalyst for epoxidation of alkenes with hydrogen peroxide. *J Am Chem Soc* 1994;116:5509–10.
- [14] Yang Y, Wu QY, Guo YH, Hu CW, Wang EB. Efficient degradation of dye pollutants on nanoporous polyoxotungstate–anatase composite under visible-light irradiation. *J Mol Catal A Chem* 2005;225:203–12.
- [15] Haimov A, Nemmann R. Polyethylene glycol as a non-ionic liquid solvent for polyoxometalate catalyzed aerobic oxidation. *Chem Commun* 2002;8:876–7.
- [16] Neumann R, Cohen M. Solvent-anchored supported liquid phase catalysis: polyoxometalate-catalyzed oxidations. *Angew Chem Int Ed Engl* 1997;36:1738–40.
- [17] Cohen M, Neumann R. Silica tethered with poly(ethylene and/propylene) oxide as supports for polyoxometalates in catalytic oxidation. *J Mol Catal A* 1999;146:291–8.
- [18] Sloboda-Rozner D, Alsters P, Neumann R. A water-soluble and “self-assembled” polyoxometalate as a recyclable catalyst for oxidation of alcohols in water with hydrogen peroxide. *J Am Chem Soc* 2003;125:5280–1.
- [19] Wang XH, Liu JF, Pope MT. New polyoxometalate/starch nanomaterial: synthesis, characterization and antitumoral activity. *Dalton Trans* 2003;5:957–60.
- [20] Wang XH, Li F, Liu SX, Pope MT. New liposome-encapsulated-polyoxometalates: synthesis and antitumoral activity. *J Inorg Biochem* 2005;99:452–7.
- [21] Mann S. Biomimetalization: principles and concepts in bioinorganic materials chemistry. Oxford: Oxford University Press; 2001.
- [22] Huang JG, Kunitake T. Nano-precision replication of natural cellulosic substances by metal oxides. *J Am Chem Soc* 2003;125:11834–5.
- [23] Huang JG, Kunitake T, Onoue S. A facile route to a highly stabilized hierarchical hybrid of titania nanotube and gold nanoparticle. *Chem Commun* 2004;8:1008–9.
- [24] Easton JR. Part I: the problem of color, the dye maker's view. In: Copper P, editor. *Color in dyehouse effluent*. Oxford: The Society of Dyes and Colourists, Alden Press; 1995. p. 9–21.
- [25] Slokar YM, Le Marechal AM. Methods of decoloration of textile wastewaters. *Dyes Pigments* 1998;37:335–56.
- [26] Rocciccioli-Deltcheff C, Frank M, Thouvenot R. Vibrational investigations of polyoxometalates 2. Evidence for anion–anion interactions in molybdenum(VI) and tungsten(VI) compounds related to the Keggin structure. *Inorg Chem* 1983;22:207–16.
- [27] Massart R, Contant R, Fruchart JM, Ciabrin JP, Fournier M. Phosphorus-31 NMR studies on molybdenic and tungstic heteropolyanions correlation between structure and chemical shift. *Inorg Chem* 1977;16:2916–21.